

A dark-line two-dimensional magneto-optical trap of 85Rb atoms with high optical depth

Shanchao Zhang, J. F. Chen, Chang Liu, Shuyu Zhou, M. M. T. Loy et al.

Citation: *Rev. Sci. Instrum.* **83**, 073102 (2012); doi: 10.1063/1.4732818

View online: <http://dx.doi.org/10.1063/1.4732818>

View Table of Contents: <http://rsi.aip.org/resource/1/RSINAK/v83/i7>

Published by the [American Institute of Physics](#).

Related Articles

Low power field generation for magneto-optic fiber-based interferometric switches
[J. Appl. Phys. 111, 07A941 \(2012\)](#)

Multi-scale/multi-physical modeling in head/disk interface of magnetic data storage
[J. Appl. Phys. 111, 07B712 \(2012\)](#)

TetraMag: A compact magnetizing device based on eight rotating permanent magnets
[Rev. Sci. Instrum. 83, 025109 \(2012\)](#)

Optical and magneto-optical properties of one-dimensional magnetized coupled resonator plasma photonic crystals
[Phys. Plasmas 19, 012503 \(2012\)](#)

Hybrid magneto-optical mode converter made with a magnetic nanoparticles-doped $\text{SiO}_2/\text{ZrO}_2$ layer coated on an ion-exchanged glass waveguide
[Appl. Phys. Lett. 99, 251108 \(2011\)](#)

Additional information on *Rev. Sci. Instrum.*

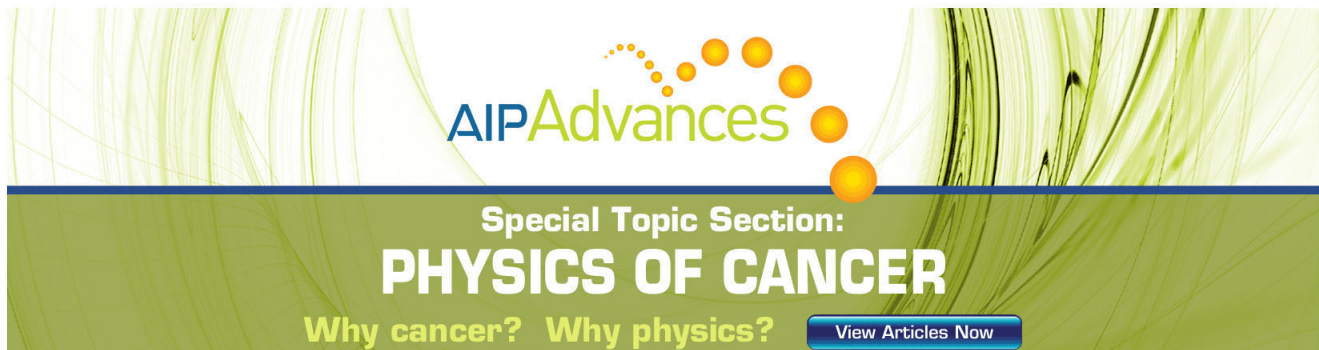
Journal Homepage: <http://rsi.aip.org>

Journal Information: http://rsi.aip.org/about/about_the_journal

Top downloads: http://rsi.aip.org/features/most_downloaded

Information for Authors: <http://rsi.aip.org/authors>

ADVERTISEMENT



The advertisement banner features a green and yellow abstract background with flowing lines. At the top center, the text "AIPAdvances" is displayed in a green, sans-serif font, with a series of yellow and orange circles of varying sizes arranged in an arc above it. Below this, the text "Special Topic Section:" is written in a smaller, white, sans-serif font. Underneath, the words "PHYSICS OF CANCER" are prominently displayed in a large, bold, white, sans-serif font. At the bottom left, the phrase "Why cancer? Why physics?" is written in a yellow, sans-serif font. At the bottom right, there is a blue button with the text "View Articles Now" in white.

A dark-line two-dimensional magneto-optical trap of ^{85}Rb atoms with high optical depth

Shanchao Zhang, J. F. Chen,^{a)} Chang Liu, Shuyu Zhou, M. M. T. Loy, G. K. L. Wong, and Shengwang Du^{b)}

Department of Physics, The Hong Kong University of Science and Technology, Clear Water Bay, Kowloon, Hong Kong, China

(Received 19 April 2012; accepted 17 June 2012; published online 10 July 2012)

We describe the apparatus of a dark-line two-dimensional (2D) magneto-optical trap (MOT) of ^{85}Rb cold atoms with high optical depth (OD). Different from the conventional configuration, two (of three) pairs of trapping laser beams in our 2D MOT setup do not follow the symmetry axes of the quadrupole magnetic field: they are aligned with 45° angles to the longitudinal axis. Two orthogonal repumping laser beams have a dark-line volume in the longitudinal axis at their cross over. With a total trapping laser power of 40 mW and repumping laser power of 18 mW, we obtain an atomic OD up to 160 in an electromagnetically induced transparency (EIT) scheme, which corresponds to an atomic-density-length product $NL = 2.05 \times 10^{15} \text{ m}^{-2}$. In a closed two-state system, the OD can become as large as more than 600. Our 2D MOT configuration allows full optical access of the atoms in its longitudinal direction without interfering with the trapping and repumping laser beams spatially. Moreover, the zero magnetic field along the longitudinal axis allows the cold atoms maintain a long ground-state coherence time without switching off the MOT magnetic field, which makes it possible to operate the MOT at a high repetition rate and a high duty cycle. Our 2D MOT is ideal for atomic-ensemble-based quantum optics applications, such as EIT, entangled photon pair generation, optical quantum memory, and quantum information processing. © 2012 American Institute of Physics. [<http://dx.doi.org/10.1063/1.4732818>]

I. INTRODUCTION

Laser cooling and trapping of neutral atoms has become a standard technology in the research field of modern atomic, molecular and optical physics,^{1,2} as well as in physics education laboratories.³ As the most common laser cooling method, the magneto-optical trap (MOT), since the first demonstration in 1987,⁴ has been widely applied on many fundamental and practical researches, such as precision spectroscopy,⁵ atomic clock,⁶ atom interferometry,^{7,8} and cold atomic collision.^{9–11} More importantly, it paved the way for creating Bose-Einstein condensates (BEC) for the first time at laboratory in 1995.^{12,13}

The temperature of cold atoms in a MOT, typically ranging from tens to hundreds micron Kelvin (μK), in which the inhomogeneous Doppler broadening is negligible as compared to the atomic natural linewidth, is ideal for studying photon-atom interactions at quantum mechanics level without requiring further complicated sub- μK cooling techniques. Recently, many research efforts have been explored in using cold atoms in MOT to control and manipulate quantum interaction between photons and atoms, such as electromagnetically induced transparency (EIT),^{14,15} low-light level nonlinear optics,^{16–18} optical storage,¹⁹ and entangled photon pair generation.^{20–22} Motivated by the Duan, Lukin, Cirac, and Zoller (DLCZ) protocol,²³ cold atomic ensembles trapped in

MOTs with the EIT configuration may act as standard quantum repeaters and nodes in a long-distance quantum communication network.^{24–34} To efficiently generate and store quantum entanglement and photonic states, the cold atomic ensembles are required to operate at high optical depths (OD). For example, the theory predicted that the atomic quantum memory storage efficiency approaches unity at $\text{OD} > 100$ which is crucial to a practical quantum network and quantum information processing.³⁵ A practical EIT system with the delay-bandwidth product more than 2 can only be obtainable as $\text{OD} > 40$.^{36,37} In most cold atom related quantum optics experiments, high atomic OD is preferred because the strong photon-atom interaction at a single-photon level depends on the atomic collective enhancement. Meanwhile, to have a long atomic ground-state coherence time, one must switch off the MOT trapping laser fields during the application window. As a result, the MOT trapping time and application window have to be put into different time slots periodically. Therefore, a MOT with a high OD, high repetition rate, and large duty cycle is desirable for quantum optics applications, especially for those working with single photon states.

However, the conventional three-dimensional (3D) MOT, which has been widely implemented for the above mentioned EIT-related quantum optics researches,^{20–22,24–34} has a typical low OD of about 10. The OD can be further increased as one applies additional cooling process, such as polarization gradient cooling³⁸ and forced evaporative cooling.¹² However, these additional cooling processes require relatively long time (from several hundred ms to seconds) that dramatically reduces the duty cycle of the atoms. For example, high OD

^{a)}Present address: Department of Physics, East China Normal University, Shanghai 200062, People's Republic of China.

^{b)}Author to whom correspondence should be addressed. Electronic mail: dusw@ust.hk.

can be achieved at or close to the BEC transition temperature and was used for observing ultra slow light effect and coherent optical information storage.^{39,40} However, a BEC, which typically requires more than 10 s atomic state preparation time, is not practical for single-photon quantum state operations due to its low duty cycle and repetition rate. Most recently, a high repetition rate BEC production with a period of 2.65 s was realized in a compact atom-chip system,⁴¹ which is still too slow for photon counting experiments. A better solution to obtain high OD (>100) in the 3D MOT is producing a cigar-shaped atom cloud with the dark-spot MOT configuration.^{42–44} However, like all 3D MOTs, it is still required to switch off the MOT magnetic fields. Usually the speed of switching on and off magnetic field is slow due to the inductance of the magnetic coils. Meanwhile, the background stray fields need to be compensated in a complicated way.⁴⁵

This problem may be solved by using the two-dimensional (2D) MOT configuration, where atoms are cooled and trapped along the zero-field line (or called the longitudinal axis) of a 2D quadrupole magnetic field and a long ground-state coherence time can be maintained without switching off the magnetic field. However, in the conventional 2D MOT with four trapping laser beams,^{46–48} there is no cooling and trapping along the longitudinal axis and the atoms can move freely along the line. This 2D MOT is often used to produce moving atomic flux, but not for a stable trap. This problem can be overcome by adding a third pair of counter-propagating trapping beam along the longitudinal axis.^{49,50} Indeed a stable trap is formed in this six-beam 2D MOT, but the two beams along the longitudinal axis are in the way of optical access along the high OD direction.

In this paper, we review and describe a modified and improved dark-line 2D MOT apparatus in which we are able to not only produce cold atoms with high OD (>100) but also obtain a low ground-state dephasing rate ($2\pi \times 0.03$ MHz) without switching off the quadrupole magnetic field. Different from the conventional setup, two pair trapping laser beams do not follow the symmetry axes of the quadrupole magnetic field: they are aligned with 45° angles relative to the longitudinal axis of the MOT. Two orthogonal repumping laser beams have a dark-line volume in the longitudinal axis at their cross over. Because the trapping and repumping laser beams are spatially separated from the longitudinal axis, they can be controlled by high speed acousto-optic modulators (AOM) and electro-optic modulators. The MOT can be operated at a high repetition rate. With total trapping laser power of 40 mW and repumping laser power of 18 mW, we obtain an atomic OD up to 160 in an EIT transition. The low ground-state dephasing rate of about $2\pi \times 0.03$ MHz meets the requirement of most EIT applications. In the past three years, this apparatus without the dark line has been used for many high quality EIT-based quantum optics researches, including the generation and manipulation of subnatural linewidth entangled photon pairs,^{52–56} experimental observation of optical precursors in both coherent light pulses and single photon wave packets.^{57–59} Most recently, the 2D MOT with dark line was applied for efficient optical storage.⁶⁰ Our 2D MOT with tunable OD will find important

application in atomic-ensemble-based quantum communication and quantum information processing.

II. 2D MOT SETUP

A typical MOT apparatus comprises an ultra-high vacuum (UHV) cell, magnetic fields, and laser beams. We use an octagonal glass cell, which is customized from Technical Glass Inc, as the MOT chamber. The vacuum system is constructed following the standard UHV technology which we will not describe in details in this review. We install totally 4 rubidium (Rb) dispensers (SAES, RB/NF/4.8/17 FT10+10) to provide controllable Rb vapor pressure. During the MOT operation, we only run two dispensers and the other two are reserved for backup. By tuning the current of two dispensers in series, the Rb vapor pressure can be changed from 10^{-10} to 10^{-7} Torr. The naturally occurring rubidium is composed of ^{85}Rb (72.2%) and ^{87}Rb (27.8%). In this work, we describe the 2D MOT for ^{85}Rb atoms, but the system can also be used to cool and trap ^{87}Rb atoms by changing the MOT laser frequencies. The principle described here can also be applied to other alkali atoms. We have two modes to operate the 2D MOT. They are the dark-line 2D MOT and the 2D MOT without dark line.

A. Dark-line 2D MOT

The schematics of our dark-line 2D MOT setup and ^{85}Rb atomic energy level diagram are shown in Fig. 1, where the vacuum cell is not shown. As illustrated in Fig. 1(a), the magneto-optical configuration comprises a 2D quadrupole magnetic field produced from a magnetic coil, six trapping beams, and two repumping beams with an overlapped dark line. The magnetic coil is constructed from a single copper wire with a square cross section (5×5 mm) and hollow core. The coil is designed for obtaining short switching on/off time with a low inductance at a high current up to 200 A. The operating current is 70 A for the 2D MOT experiment described in this work. The magnetic coil is cooled by water flux through the hollow core. This 3D coil structure can be considered as a cage surrounded by four single-loop coils, but the single-wire coil design minimizes the number of electric connections, and more importantly, it minimizes the number of water connections. As discussed later, when there is no need to switch off the MOT magnetic field, we can replace the coil with a four-coil set with multiple turns so that high current and water cooling are not necessary. From the coil symmetry, the generated 2D quadrupole magnetic field has a zero field line along the longitudinal z axis. The 2D magnetic field pattern on x - y plane is displayed in Fig. 1(b). The trapping laser is red detuned by 20 MHz from the transition $|5S_{1/2}, F=3\rangle \rightarrow |5P_{3/2}, F=4\rangle$, and the repumping laser is on resonance with the transition $|5S_{1/2}, F=2\rangle \rightarrow |5P_{3/2}, F=2\rangle$. Both trapping and repumping beams have the same beam diameter of 2 cm. One pair of counterpropagating trapping laser beams (1 and 2) are aligned along the x axis. Different from the conventional 2D and 3D MOT optical alignments, the other four trapping beams are not aligned along the symmetry axes of the magnetic field. For example, in the conventional 2D MOT configuration,^{49,50} these four

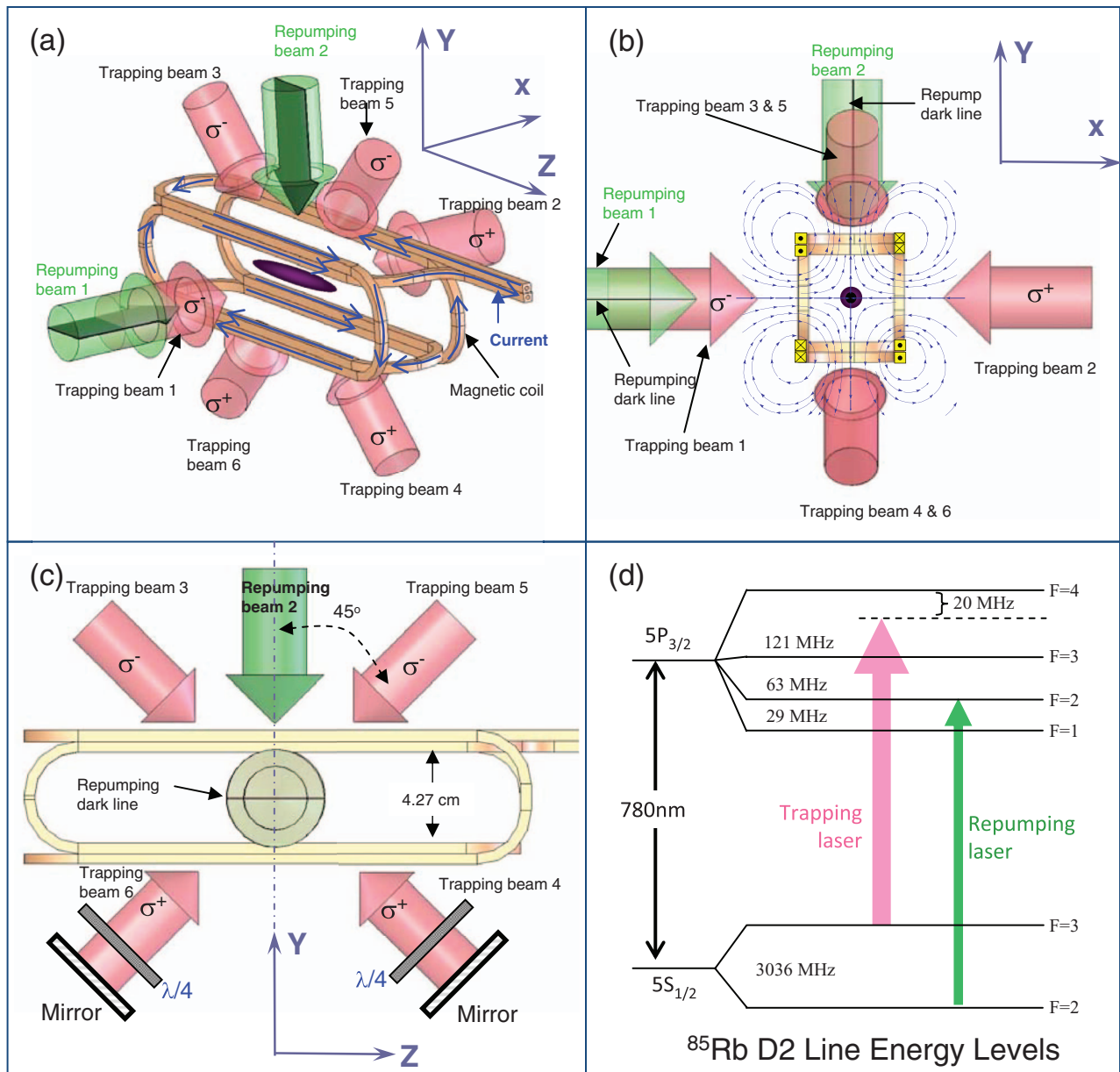


FIG. 1. Schematics of the dark-line 2D MOT magneto-optical configuration. (a) is a 3D view. (b) and (c) are cross section views in x-y and y-z planes, respectively. (d) is the ^{85}Rb D₂ line energy level diagram with MOT laser transitions.

trapping beams are aligned along y and z axes. However, in our 2D MOT setup, we align these four trapping beams (3, 4, 5, and 6) at 45° angles to the y and z axes, as shown in Fig. 1(c). Because the atoms are trapping along the longitudinal z axis, this configuration opens full optical access along the atom line which is the direction for high OD. With the illustrated magnetic coil current direction and magnetic field, the polarizations (σ^+ and σ^-) of the six trapping beams are also shown in Figs. 1(a)–1(c). To efficiently make use of the trapping laser power, the two 45° beams are retro reflected as shown in Fig. 1(c). We use two repumping laser beams. The repumping beam 1 overlaps with the trapping beam 1 along the x axis. the repumping beam 2 is aligned along the y axis. In each repumping beam, there is a copper wire line with a diameter of 0.6 mm. The images of these copper wires with a unit magnification, through a 4f lens system in

each beam, overlap at the center of the 2D MOT and create a dark line (with a square cross section of 0.6×0.6 mm) of the repumping beams along the z axis. In the dark line regime, the atoms are pumped into the dark state $|5S_{1/2}, F=2\rangle$ without interacting with the trapping laser and thus avoid the radiation trapping loss and heating. As an extension of the dark-spot 3D MOT, the dark line can significantly increase the atomic density and optical depth. In the dark-line 2D MOT, we obtain OD in an EIT transition up to 160, with a trapping laser power of only 40 mW and a repumping laser power of 18 mW.

B. 2D MOT without dark line

If an OD of less than 50 is enough for application, one can work with the 2D MOT without the dark line in which

the optical alignment can be simplified. In this mode, one can remove the copper wires as well as the imaging lenses in the two repumping beams. To open more optical access along the y axis, one can also remove the repumping beam 2 and put all the repumping laser power to its beam 1. This 2D MOT is robust and very easy to setup.

C. Magnetic coil design

The water-cooled magnetic coil shown in Fig. 1 is made of a single hollow-core copper wire with a square cross section. We obtain a transverse magnetic field gradient of 10 G/cm with a current of 70 A for the MOT. The small inductance ($\sim 100 \mu\text{H}$) of this coil also allows us to switch on and off the magnetic field in a short time. Controlling the magnetic field is necessary for obtaining the atomic ground state coherence time of more than 10 μs . We obtain a dephasing rate of $\gamma_{12} = 2\pi \times 0.03$ MHz between the two ground levels ($|1\rangle = |5S_{1/2}, F=2\rangle$ and $|2\rangle = |5S_{1/2}, F=3\rangle$), which corresponds to a coherence time of $\tau_{12} = 5.3 \mu\text{s}$, without switching off the 2D MOT quadruple magnetic field during the measurement. If such several μs coherence time is long enough for applications, the quadruple magnetic field can be remained on all the time and the magnetic coil can be simplified. In this case, the magnetic coil set can be assembled from four independent coils, as shown in Fig. 2(a). There are multiple turns in each coil so that they can be driven by a low current power supply without water cooling. Such a steady MOT magnetic field can also be generated from 4 permanent magnet bars aligned in the configuration shown in Fig. 2(b).⁴¹ Using permanent magnetic magnets dramatically simplify the system and reduce the power consumption because it can be self-standing without using any electrical power supply.

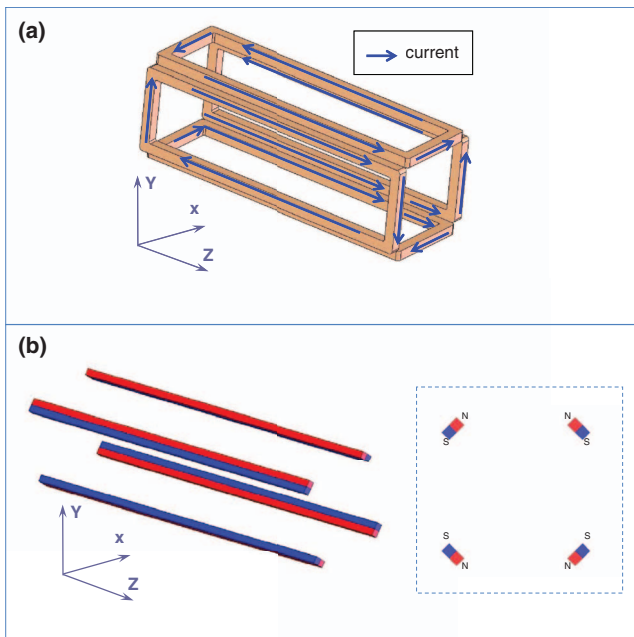


FIG. 2. Two alternative ways to produce a steady 2D MOT quadruple magnetic field: (a) A magnetic coil set with many turns, and (b) a permanent magnet set. The inset inside (b) shows the alignment of the 4 magnets in x - y plane.

III. EIT AND MEASUREMENT

Figure 3 shows two fluorescence pictures of cold atoms in the 2D MOT, with a longitudinal length of 1.7 cm and an aspect ratio of about 25. We take EIT measurements to characterize the 2D MOT properties. EIT,¹⁴ as a quantum interference between atomic transitions, has been widely used to manipulate optical response of an atomic medium, and found its wide applications in slow light,³⁹ nonlinear wave mixing,¹⁸ optical switching,^{16,17} entangled photon pair generation,^{20–22} optical quantum memory,⁵¹ and quantum information processing.²³ The EIT measurement scheme is shown in Fig. 4, where (a) is the involved energy level diagram in ^{85}Rb D1 lines (795 nm), (b) is the optical setup, and (c) is the timing. We consider an EIT Λ system in the following three levels: $|1\rangle = |5S_{1/2}, F=2\rangle$, $|2\rangle = |5S_{1/2}, F=3\rangle$, and $|3\rangle = |5P_{1/2}, F=3\rangle$. A weak probe laser (ω_p) beam propagates along the 2D MOT longitudinal z axis and is focused to the center of the MOT with a $1/e^2$ beam diameter of 245 μm at the waist. We measure the probe absorption spectrum with a photomultiplier tube (PMT, Hamamatsu, H6780-20) by scanning its frequency across the transition $|1\rangle \rightarrow |3\rangle$. To ensure that linear propagation effect is studied, we keep the intensity of the probe laser sufficiently low (~ 100 nW) that the atomic population remains primarily in the state $|1\rangle$. A collimated coupling laser beam, ω_c , on resonance at the transition $|2\rangle \rightarrow |3\rangle$ and with a $1/e^2$ beam diameter of 1.6 mm, passes through the cold atoms with an angle of 3° respect to the probe laser beam. Both the probe and coupling laser beams have the same circular polarizations (σ^+) to optimize the EIT effect. The measurement is taken periodically. At each period of $T = 5$ ms, we set the MOT trapping time $t_{\text{MOT}} = 4.2$ ms and the measurement duty (including state preparation and EIT measurement) time $t_{\text{duty}} = 0.8$ ms. At each cycle, after the repumping laser is switched off, we remain on the trapping laser for additional $\Delta t = 0.3$ ms to optically pump all the atoms into the ground state $|1\rangle$, which is preferable for the EIT scheme. To reduce this time of 0.3 ms in the duty window, one can also use an additional on-resonance laser to pump the atoms more efficiently in a much shorter time ($< 50 \mu\text{s}$). After the atoms are prepared in the ground state $|1\rangle$, we switch on the probe and/or coupling lasers for absorption measurement inside the duty window. All the laser powers are controlled by AOMs.

Under the plane-wave approximation, the transmission of the weak probe laser after passing through the EIT medium is

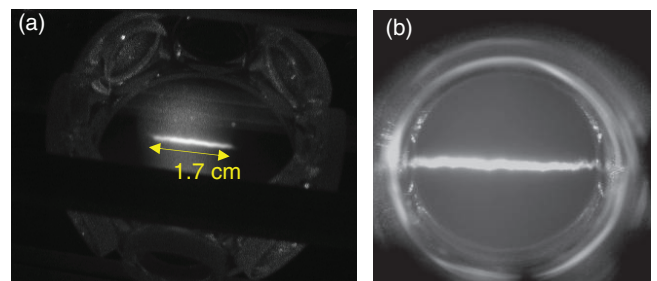


FIG. 3. Fluorescence pictures of cold atoms in the 2D MOT viewed from (a) the x direction and (b) the y direction.

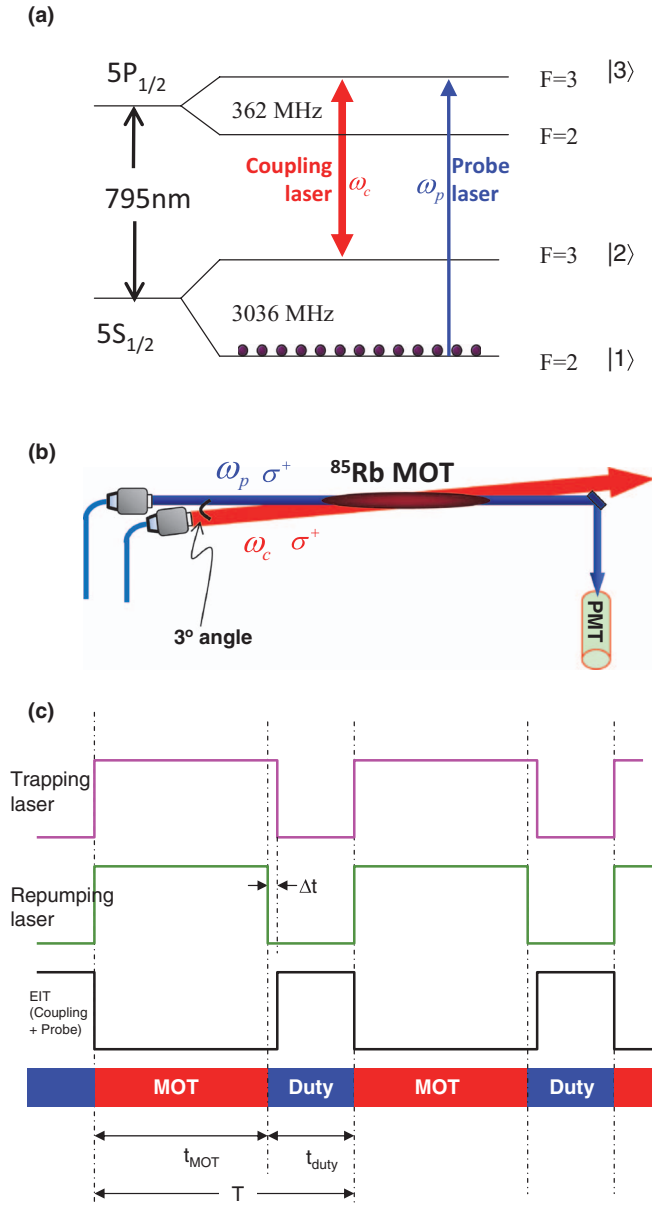


FIG. 4. EIT measurement scheme. (a) EIT atomic energy level diagram. (b) EIT measurement optical setup. (c) MOT and EIT measurement timing.

given by

$$\text{Tran}(\omega_p) = |e^{ik(\omega_p)L}|^2 = e^{-2\text{Im}[k(\omega_p)]L}, \quad (1)$$

where L is the medium length and $k(\omega_p) = (\omega_p/c)\sqrt{1 + \chi} \simeq (\omega_p/c)(1 + \chi/2)$ is the complex wave number in the medium with the speed of light in vacuum c . The EIT linear susceptibility (complex) is given as⁵⁷

$$\chi = \frac{\alpha_0}{k_0} \frac{4(\Delta\omega_p + i\gamma_{12})\gamma_{13}}{|\Omega_c|^2 - 4(\Delta\omega_p + i\gamma_{12})(\Delta\omega_p + i\gamma_{13})}, \quad (2)$$

where α_0 is the on-resonance absorption coefficient of the transition $|1\rangle \rightarrow |3\rangle$ when the coupling laser is not present, $k_0 = \omega_{31}/c$, $\Delta\omega_p = \omega_p - \omega_{31}$ is the probe detuning, and Ω_c is the coupling laser Rabi frequency. The atomic-lifetime-determined electric dipole relaxation rate between $|1\rangle$ and $|3\rangle$ is $\gamma_{13} = 2\pi \times 3$ MHz. When the coupling laser is switched off ($\Omega_c = 0$), Eq. (2) reduces to that of a two-level system.

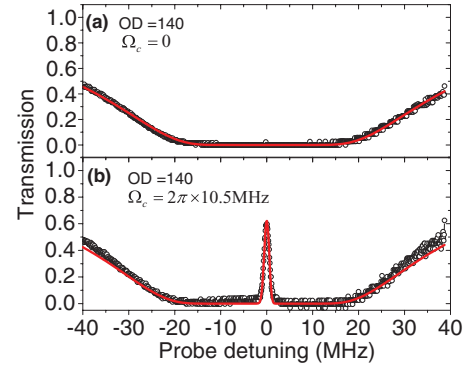


FIG. 5. The probe absorption spectrum profile at $OD = 140$ in (a) a two-level system ($\Omega_c = 0$) and (b) an EIT system ($\Omega_c = 2\pi \times 10.5$ MHz). The circular points are experimental data, and the solid are theoretical curves plotted from Eq. (1).

The atomic optical depth $OD = \alpha_0 L$ and ground-state dephasing rate γ_{12} are obtained as the best fitting parameters of Eq. (1) to the measurement data.

Figure 5 shows typical absorption measurement results of the dark-line 2D MOT. As discussed previously, when the coupling laser is not present ($\Omega_c = 0$), the EIT reduces to a two-level system and the probe laser gets maximally absorbed on resonance, shown in Fig. 5(a). When the coupling laser is switched on ($\Omega_c = 2\pi \times 10.5$ MHz), it renders the medium a narrow transparent window around the resonance, as shown in Fig. 5(b). The solid curves are the best fitting of Eq. (1) to the experimental data, and we obtain $OD = 140$ and $\gamma_{12} = 2\pi \times 0.03$ MHz.

Figure 6 shows the measured OD as a function of the current of two dispensers. We operate the 2D MOT with a trapping laser power of 80 mW and a repumping laser power of 18 mW. When the 2D MOT is operated without the dark line, we find the OD reaches a saturation value of 60 as the current approaches 3.5 A, as shown in plot (1) of Fig. 6. In the dark-line 2D MOT configuration, we observe a significant increase of OD to 130 at a high dispenser current [plot (2) of Fig. 6]. During the measurement, we find that the repumping beam is not completely dark at the dark line due to scattering, diffraction, and the imperfectness of the imaging system. To solve this problem, we turn on the coupling laser during the MOT time at a very weak power of $10 \mu\text{W}$ to act as a

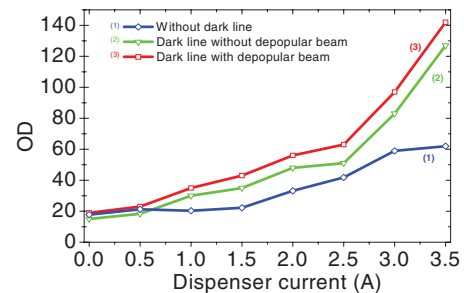


FIG. 6. The measured OD as a function of the current of two dispensers in (1) the 2D MOT without the dark line, and the dark-line 2D MOT (2) without the depopular beam and (3) with the depopular beam. In these sets of measurements, we operate the 2D MOT with a trapping laser power of 80 mW and a repumping laser power of 18 mW.

depopular beam. The measured OD with the depopular beam is shown in plot (3) of Fig. 6, and we observe a slight increase of OD from 130 to 140 at the dispenser current of 3.5 A. A higher OD is achievable at a larger dispenser current. Because the depopular beam only increases the OD slightly, in the following measurements and discussions, we work only with the dark-line 2D MOT without the depopular beam.

We then study the dependence of OD on the trapping and repumping laser powers, in the dark-line 2D MOT configuration without the depopular beam. At first, we fix the repumping laser power at 18 mW and vary the trapping laser power. Figure 7(a) shows the measured OD as a function of the trapping laser power. At a low power, the OD increases linearly as the trapping laser power. It reaches a saturation value as we increase the trapping laser power to more than 30 mW. The slight decrease of OD at high trapping laser power may be caused by the power unbalancing between the six trapping laser beams. We then set the trapping laser power at 40 mW and vary the repumping laser power. The measured OD vs repumping laser power is shown in Fig. 7(b). The OD starts to saturate at a repumping laser power of 3 mW. As a result, we obtain OD = 160 in the dark-line 2D MOT with a low trapping laser power of only 40 mW. Such a low laser power requirement may drastically reduce the complicity of the laser system.

Another important number for characterizing the system performance is the duty cycle, defined as the ratio of duty window time length to the period

$$\eta = \frac{t_{duty}}{T}. \quad (3)$$

Because the MOT time and EIT application duty window must be separated at different time slots, the duty cycle

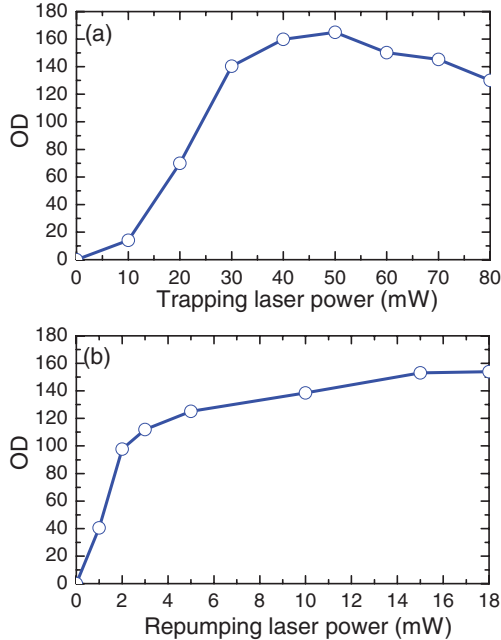


FIG. 7. The measured OD as a function of the power of the trapping and repumping lasers in the dark-line 2D MOT. (a) OD vs trapping laser power when the repumping laser power is fixed at 18 mW. (b) OD vs repumping laser power when the trapping laser power is fixed at 40 mW.

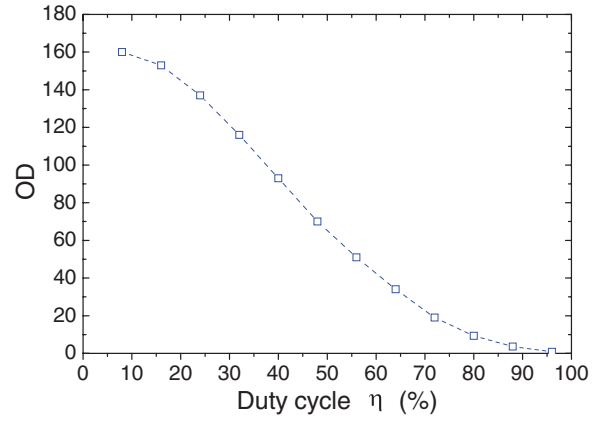


FIG. 8. The measured OD in the dark-line 2D MOT (without the depopular beam) as a function of the duty cycle.

reflects the use efficiency of the cold atoms. During the duty window, we lose some atoms from the trap because of the background collision, free expansion, and falling under the gravity. As a result, the optical depth drops as we increase the duty cycle. The above measurements are taken with a duty cycle $\eta = 16\%$. The duty cycle can be varied by changing either the MOT trapping time t_{MOT} and or the duty time t_{duty} . Figure 8 shows the measured OD as a function of duty cycle at the dispenser current of 3.5 A, with the lasers operated at 40 mW and 18 mW for the trapping laser and repumping laser, respectively. As we increase the duty cycle to 35%, we still have OD more than 100. For most applications where an OD of about 50 is enough, we can run the 2D MOT with a duty cycle of 55%. If an OD of 10 is needed, we can increase the duty cycle up to 80%.

We must mention that the OD discussed previously is in the EIT three-level scheme where $|1\rangle \rightarrow |3\rangle$ is an open transition with an absorption cross section $\sigma_{13} = \frac{7}{27} \times \frac{3\lambda_p^2}{2\pi}$. Here λ_p is the on-resonance probe laser wavelength. With the atomic density N , the optical depth can be expressed as $OD = \alpha_0 L = N\sigma_{13}L$. Therefore, the product of atomic density N and length L is independent of the transition strength of the chosen states. At OD = 160, we get $NL = 2.05 \times 10^{15} \text{ m}^{-2}$. In a closed two-state system, such as $|5S_{1/2}, F = 3, M_F = 3\rangle \rightarrow |5P_{3/2}, F = 4, M_F = 4\rangle$, the absorption cross section becomes $\sigma_0 = \frac{3\lambda_p^2}{2\pi}$ and we can get an OD of more than 600.

IV. SUMMARY

In summary, we have described the apparatus of dark-line 2D MOT of ^{85}Rb atoms and its EIT measurements. In our six-trapping-beam optical setup, four trapping beams are aligned with 45° angles to the longitudinal axis and do not follow the conventional setup along the symmetry axes. We use two orthogonal repumping laser beams with a dark-line volume in the longitudinal axis at their cross over. This trapping-repumping beam configuration opens full optical access along the longitudinal axis and it is important for quantum optics experiments. With a total trapping laser power of 40 mW and repumping power of 18 mW, we obtain cold atoms with a high OD of up to 160, which corresponds to $NL = 2.05 \times 10^{15} \text{ m}^{-2}$. In a simplified configuration without the dark

line, the 2D MOT is capable to have OD up to 60. In a closed two-state system, we can get the OD up to more than 600. Because the atoms are trapped along the zero magnetic field line in the longitudinal z axis, we obtain a low ground-state dephasing rate $\gamma_{12} = 2\pi \times 0.03$ MHz with the MOT magnetic field remaining on. It greatly simplifies the system operation without the need of turning off the MOT magnetic field and allows the MOT operated at a high repetition rate and a high duty cycle. In this work, we describe the 2D MOT for ^{85}Rb atoms, but the system can also be used to trap ^{87}Rb atoms by changing the MOT laser frequencies. The principle described here works also for other alkali atoms. Since 2008, this 2D MOT without dark line has been applied in generating narrow-band entangled photon pairs,^{52–56} and the observation of optical precursors at both coherent light pulses and single photons.^{57–59} Most recently, We use the dark-line 2D MOT with a high optical depth to study EIT optical storage.⁶⁰ Our 2D MOT at a high optical depth with a low trapping laser power provides a nearly ideal cold atom source for EIT-related quantum optics research and may find important applications in atomic-ensemble-based quantum networks.

ACKNOWLEDGMENTS

The work was supported by the Hong Kong Research Grants Council (Project Nos. 600710, DAG_S09/10.SC06 and DAG08/09.SC02).

- ¹H. J. Metcalf and P. V. der Straten, *Laser Cooling and Trapping* (Springer, 1999).
- ²W. D. Phillips, *Rev. Mod. Phys.* **70**, 721 (1998).
- ³A. S. Mellish and A. C. Wilson, *Am. J. Phys.* **70**, 965 (2002).
- ⁴E. L. Raab, M. Prentiss, A. Cable, S. Chu, and D. E. Pritchard, *Phys. Rev. Lett.* **59**, 2631 (1987).
- ⁵J. W. R. Tabosa, G. Chen, Z. Hu, R. B. Lee, and H. J. Kimble, *Phys. Rev. Lett.* **66**, 3245 (1991).
- ⁶M. M. Boyd, A. D. Ludlow, S. Blatt, S. M. Foreman, T. Ido, T. Zelevinsky, and J. Ye, *Phys. Rev. Lett.* **98**, 083002 (2007).
- ⁷M. Kasevich and S. Chu, *Phys. Rev. Lett.* **67**, 181 (1991).
- ⁸M. J. Snadden, J. M. McGuirk, P. Bouyer, K. G. Haritos, and M. A. Kasevich, *Phys. Rev. Lett.* **81**, 971 (1998).
- ⁹D. Sesko, T. Walker, C. Monroe, A. Gallagher, and C. Wieman, *Phys. Rev. Lett.* **63**, 961 (1989).
- ¹⁰D. Hoffmann, P. Feng, R. S. Williamson, and T. Walker, *Phys. Rev. Lett.* **69**, 753 (1992).
- ¹¹J. Weiner, V. S. Bagnato, S. Zilio, and P. S. Julienne, *Rev. Mod. Phys.* **71**, 1 (1999).
- ¹²M. H. Anderson, J. R. Ensher, M. R. Matthews, C. E. Wieman, and E. A. Cornell, *Science* **269**, 198 (1995).
- ¹³K. B. Davis, M.-O. Mewes, M. R. Andrews, N. J. van Druten, D. S. Durfee, D. M. Kurn, and W. Ketterle, *Phys. Rev. Lett.* **75**, 3969 (1995).
- ¹⁴S. E. Harris, *Phys. Today* **50**(7), 36 (1997).
- ¹⁵M. Fleischhauer, A. Imamoglu, and J. P. Marangos, *Rev. Mod. Phys.* **77**, 633 (2005).
- ¹⁶M. Yan, E. G. Riskey, and Y. Zhu, *Phys. Rev. A* **64**, 041801(R) (2001).
- ¹⁷D. A. Braje, V. Balić, G. Y. Yin, and S. E. Harris, *Phys. Rev. A* **68**, 041801(R) (2003).
- ¹⁸D. A. Braje, V. Balić, S. Goda, G. Y. Yin, and S. E. Harris, *Phys. Rev. Lett.* **93**, 183601 (2004).
- ¹⁹Y. F. Chen, P. C. Kuan, S. H. Wang, C. Y. Wang, and I. A. Yu, *Opt. Lett.* **31**, 3511 (2006).
- ²⁰V. Balić, D. A. Braje, P. Kolchin, G. Y. Yin, and S. E. Harris, *Phys. Rev. Lett.* **94**, 183601 (2005).
- ²¹P. Kolchin, S. Du, C. Belthangady, G. Y. Yin, and S. E. Harris, *Phys. Rev. Lett.* **97**, 113602 (2006).
- ²²S. Du, J. Wen, M. H. Rubin, and G. Y. Yin, *Phys. Rev. Lett.* **98**, 053601 (2007).
- ²³L. M. Duan, M. D. Lukin, J. I. Cirac, and P. Zoller, *Nature (London)* **414**, 413 (2001).
- ²⁴A. Kuzmich, W. P. Bowen, A. D. Boozer, A. Boca, C. W. Chou, L. M. Duan, and H. J. Kimble, *Nature (London)* **423**, 731 (2003).
- ²⁵C. W. Chou, S. V. Polyakov, A. Kuzmich, and H. J. Kimble, *Phys. Rev. Lett.* **92**, 213601 (2004).
- ²⁶D. N. Matsukevich and A. Kuzmich, *Science* **306**, 663 (2004).
- ²⁷D. N. Matsukevich, T. Chanelière, M. Bhattacharya, S.-Y. Lan, S. D. Jenkins, T. A. B. Kennedy, and A. Kuzmich, *Phys. Rev. Lett.* **95**, 040405 (2005).
- ²⁸C. W. Chou, H. de Riedmatten, D. Felinto, S. V. Polyakov, S. J. van Enk, and H. J. Kimble, *Nature (London)* **438**, 828 (2005).
- ²⁹D. Matsukevich, T. Chanelière, S. D. Jenkins, S.-Y. Lan, T. A. B. Kennedy, and A. Kuzmich, *Phys. Rev. Lett.* **96**, 030405 (2006).
- ³⁰S. D. Jenkins, D. N. Matsukevich, T. Chanelière, S.-Y. Lan, T. A. B. Kennedy, and A. Kuzmich, *J. Opt. Soc. Am. B* **24**, 316 (2007).
- ³¹C. W. Chou, J. Laurat, H. Deng, K. S. Choi, H. de Riedmatten, D. Felinto, and H. J. Kimble, *Science* **316**, 1316 (2007).
- ³²J. Laurat, K. S. Choi, H. Deng, C. W. Chou, and H. J. Kimble, *Phys. Rev. Lett.* **99**, 180504 (2007).
- ³³K. S. Choi, H. Deng, J. Laurat, and H. J. Kimble, *Nature (London)* **452**, 67 (2008).
- ³⁴K. S. Choi, A. Goban, S. B. Papp, S. J. van Enk, and H. J. Kimble, *Nature (London)* **468**, 412 (2010).
- ³⁵A. V. Gorshkov, A. André, M. Fleischhauer, A. S. Sørensen, and M. D. Lukin, *Phys. Rev. Lett.* **98**, 123601 (2007).
- ³⁶S. E. Harris and L. V. Hau, *Phys. Rev. Lett.* **82**, 4611 (1999).
- ³⁷S. Du, J. Wen, and M. H. Rubin, *J. Opt. Soc. Am. B* **25**, C98 (2008).
- ³⁸J. Dalibard and C. Cohen-Tannoudji, *J. Opt. Soc. Am. B* **6**, 2023 (1989).
- ³⁹L. V. Hau, S. E. Harris, Z. Dutton, and C. H. Behroozi, *Nature (London)* **397**, 594 (1999).
- ⁴⁰C. Liu, Z. Dutton, C. H. Behroozi, and L. V. Hau, *Nature (London)* **409**, 490 (2001).
- ⁴¹M. B. Squires, “High repetition rate Bose-Einstein condensate production in a compact, transportable vacuum system,” Ph.D. dissertation, University of Colorado at Boulder, 2008.
- ⁴²W. Ketterle, K. B. Davis, M. A. Joffe, A. Martin, and D. E. Pritchard, *Phys. Rev. Lett.* **70**, 2253 (1993).
- ⁴³Y.-W. Lin, H.-C. Chou, P. P. Dwivedi, Y.-C. Chen, and I. A. Yu, *Opt. Express* **16**, 3753 (2008).
- ⁴⁴A. G. Radnaev, Y. O. Dudin, R. Zhao, H. H. Jen, S. D. Jenkins, A. Kuzmich, and T. A. B. Kennedy, *Nat. Phys.* **6**, 894 (2010).
- ⁴⁵D. Felinto, C. W. Chou, H. de Riedmatten, S. V. Polyakov, and H. J. Kimble, *Phys. Rev. A* **72**, 053809 (2005).
- ⁴⁶J. Schoser, A. Batär, R. Löw, V. Schweikhard, A. Grabowski, Y. B. Ovchinnikov, and T. Pfau, *Phys. Rev. A* **66**, 023410 (2002).
- ⁴⁷J. Catani, P. Maioli, L. De Sarlo, F. Minardi, and M. Inguscio, *Phys. Rev. A* **73**, 033415 (2006).
- ⁴⁸T. G. Tiecke, S. D. Gensemer, A. Ludewig, and J. T. M. Walraven, *Phys. Rev. A* **80**, 013409 (2009).
- ⁴⁹E. Riis, D. S. Weiss, K. A. Moler, and S. Chu, *Phys. Rev. Lett.* **64**, 1658 (1990).
- ⁵⁰K. Dieckmann, R. J. C. Spreeuw, M. Weidemüller, and J. T. M. Walraven, *Phys. Rev. A* **58**, 3891 (1998).
- ⁵¹T. Chanelière, D. N. Matsukevich, S. D. Jenkins, S.-Y. Lan, T. A. B. Kennedy, and A. Kuzmich, *Nature (London)* **438**, 833 (2005).
- ⁵²S. Du, P. Kolchin, C. Belthangady, G. Y. Yin, and S. E. Harris, *Phys. Rev. Lett.* **100**, 183603 (2008).
- ⁵³P. Kolchin, C. Belthangady, S. Du, G. Y. Yin, and S. E. Harris, *Phys. Rev. Lett.* **101**, 103601 (2008).
- ⁵⁴C. Belthangady, S. Du, C.-S. Chuu, G. Y. Yin, and S. E. Harris, *Phys. Rev. A* **80**, 031803(R) (2009).
- ⁵⁵J. F. Chen, S. Zhang, H. Yan, M. M. T. Loy, G. K. L. Wong, and S. Du, *Phys. Rev. Lett.* **104**, 183604 (2010).
- ⁵⁶H. Yan, S. Zhang, J. F. Chen, M. M. T. Loy, G. K. L. Wong, and S. Du, *Phys. Rev. Lett.* **106**, 033601 (2011).
- ⁵⁷D. Wei, J. F. Chen, M. M. T. Loy, G. K. L. Wong, and S. Du, *Phys. Rev. Lett.* **103**, 093602 (2009).
- ⁵⁸J. F. Chen, H. Jeong, L. Feng, M. M. T. Loy, G. K. L. Wong, and S. Du, *Phys. Rev. Lett.* **104**, 223602 (2010).
- ⁵⁹S. Zhang, J. F. Chen, C. Liu, M. M. T. Loy, G. K. L. Wong, and S. Du, *Phys. Rev. Lett.* **106**, 243602 (2011).
- ⁶⁰S. Zhang, S. Zhou, M. M. T. Loy, G. K. L. Wong, and S. Du, *Opt. Lett.* **36**, 4530 (2011).